Journal of Mines, Metals and Fuels, *71(12C) : 134-142; 2023. DOI: 10.18311/jmmf/2023/47252*

Print ISSN : 0022-2755

Journal of Mines, Metals and Fuels

Contents available at: *www.informaticsjournals.com/index.php/jmmf*

Preparation, Characterization and Electromagnetic Shielding Properties of Nickel-Doped Fe_3O_4/Epoxy Composites

K. S. Anu[1], K. A. Vishnumurthy[2*] and K. Natarajan[2]

[1]Department of Chemistry, Global Academy of Technology, Bengaluru 560098, Karnataka, India
[2]Department of Chemistry, R V College of Engineering, Bengaluru 560059, Karnataka, India; vishnumurthyka@rvce.edu.in

Abstract

In this proposed work, we synthesized Ni doped Fe_3O_4 ($Ni_{0.5}Fe_{2.5}O_4$) by simple co-precipitation method. The crystal structure and phase transition in the crystal lattice had been examined by FTIR and Raman spectroscopic technique. The doping of Ni into the iron oxide was characterized by X-ray diffraction (XRD) and energy dispersive X-ray analysis (EDAX). The optical properties of the nanoparticles were also studied by the UV-Visible spectroscopy. These Ni doped Fe_3O_4 particles were incorporated into the epoxy matrix in different weight percentage (5wt%, 10wt% and 15wt%). The morphological analysis was performed by Scanning Electron Microscopy (SEM) and the electromagnetic shielding properties of the composites was measured using Vector Network Analyzer (VNA) in X-band (8-12GHz) and the study revealed that the electromagnetic shielding property increases with the increase in the filler loading. The 15wt% of the filler/epoxy composite had showed highest Electromagnetic Interference (EMI) Shielding Effectiveness (SE) value of -24.46dB at around 10GHz. Hence, Ni doped Fe_3O_4 have become an efficient EMI shielding material with excellent optical properties.

Keywords: Co-Precipitation Method, EMI Shielding, Epoxy Composites, S-Parameters

1. Introduction

Today, there is a technological surge worldwide. Increasing usage of electrical and electronic devices which operates using electrical energy generates electromagnetic waves. The signal from one device interferes with the other which leads to the Electromagnetic Interference (EMI)[1,2]. These EMI affects human health genetically, metabolically, harmonically and also leads to behavioral changes[3]. The EMI also disrupts electrical, electronic and avionic industry as it leads to malfunctioning of the devices[4]. Hence, shielding of these EM waves plays the major role. The EMI shielding efficiency of the shield is ascribed to the reflection, absorption and multiple internal reflection phenomenon[5,6]. Earlier, metals had been used as EMI shielding materials because of their excellent conductivity, malleability, ductility and lustrous characteristics[7,8]. owing to their poor resistance to corrosion and weight concerns, metals were replaced by polymer composites due to their light weight, energy savings, easy processibility and corrosion resistance[8-10].

In this regard, lot of research had been carried out on epoxy resin owing to their light weight, toughness, mechanical strength, corrosion resistant property, easy processibility and thermal stability[11,12]. Epoxy is an insulator and hence need the modification to increase the electrical and optical properties[7]. In recent years, numerous investigations had made on epoxy/Fe_3O_4 composites due to their magnetic properties,

**Author for correspondence*

corrosion resistance and light weight properties. Chan et.al explained the EMI shielding behaviour of carbon fibre veil/Fe_3O_4/epoxy multiscale composites with EMI shielding effectiveness value of 51.5dB in X-band[13]. Later, Wang prepared MWCNT-Fe_3O_4@Ag/epoxy nanocomposites with high conductivity and thermal stability and obtained superior EMI SE of 35dB[12]. Further, Fe_3O_4 was decorated with graphene nanoplatelets and their epoxy composites had prepared and their EMI shielding behaviour was measured in X-band with EMI SE value of 9.6dB[14]. Recently, cotton fibre based conductive papers were prepared with the CNTs and GNPs. These conductive papers were soaked in epoxy resin with the incorporation of Fe_3O_4 nanoparticles which showed the highest EMI SE value of 33.1dB[15]. However, the Fe_3O_4 nanoparticles agglomerate in the epoxy resin which hinders the proper cross-linking of epoxy resin during curing process that results in the poor dispersion of nanoparticles in the epoxy resin matrix[16]. Various studies had been done by the researchers to overcome the problem and one such method was structural modification of Fe_3O_4 nanoparticles by doping with other metal cations[17,18]. The transition metal cation, Ni^{2+} with high conductivity, dielectric properties, optical and electrical properties, exceptional saturation magnetization and low cost had gained the attention[19]. Muhammad *et al.*, prepared Ni doped Fe_3O_4 nanoparticles by co-precipitation method for biomedical applications[20]. The excellent EMI shielding properties of Ni^{2+} cobalt nanoferrites was explained by Rezhna Kuekha[21]. The superior dielectric properties of Ni doped Fe_3O_4 nanoparticles was also studied[22]. The Ni doped Fe_3O_4 nanoparticles had been prepared by different methods such as hydrothermal[23], sol-gel method[21,24], electrochemical method[18] and co-precipitation method[19,20,25,26].

In the present work, we synthesis Ni doped Fe_3O_4 nanoparticles using the simple co-precipitation method. The characterization was done by FTIR, XRD, SEM, EDAX, Raman spectroscopy and UV-Visible spectroscopy. The electromagnetic properties were measured using VNA. However, so many work had been carried out on Ni doped Fe_3O_4 nanoparticles, no one had studied the EMI shielding behaviour of Ni doped Fe_3O_4/epoxy composite and also the obtained EMI SE value was more compare to the other reported EMI SE value on nickel ferrites.

2. Experiment

2.1. Materials and Methods

Diglycidyl ether of bisphenol A based L-12 epoxy resin and triethylenetetramine based K-6 hardener was purchased from Atul Industries Ltd. Nickel (II) nitrate hexahydrate [$Ni(NO_3)_2.6H_2O$], $FeCl_3$, $FeSO_4.7H_2O$ and NaOH were purchased from Sri Lakumi Scientifics, Bengaluru.

2.2. Preparation of Fe_3O_4 and Nickel Doped Fe_3O_4 Nanoparticles

13.9g of $FeCl_3$ and 6.75g of $FeSO_4.7H_2O$ were mixed at 70°C and stirred for 15min. Then, NaOH was added drop wise with stirring until the PH become 11 and stirred for 1hr, followed by ultrasonication for 30min. The precipitate formed was vacuum filtered and dried in hot air oven at 120°C for 1hr [27] and calcinated at 500°C for 3hours. Thus, formed Fe_3O_4 nanoparticles were stored in airtight container for further use.

The same procedure was followed for the synthesis of Ni doped Fe_3O_4 nanoparticles ($Ni_{0.5}Fe_{2.5}O_4$) by adding the required amount of $Ni(NO_3)_2.6H_2O$ (0.5 atomic %) as the precursor.

2.3. Preparation of Nickel Doped Fe_3O_4/epoxy Composites

The prepared Fe_3O_4 and $Ni_{0.5}Fe_{2.5}O_4$ nanoparticles with different weight ratios (5wt%, 10wt% and 15wt%) were suspended in the fixed amount of epoxy and kept for ageing overnight for the complete wettability of nanoparticles in the epoxy resin. The mixture was stirred magnetically at room temperature for 1hr, followed by ultrasonication at 60°C for 20min for uniform dispersion. Then, the hardener was added in stoichiometric ratio (1:10) and magnetically stirred for 30min at 70°C. The as prepared solution was casted into the aluminium moulds and kept in the hot air oven for one hr at 80°C, then post cured at 100°C for 1hour [28].

2.4. Characterization

The structural analysis of the prepared nanoparticles had been studied using (FTIR) Spectroscopy with the wavenumber ranging from 400-4000cm^{-1} which determine functional groups present in the nanoparticles. The XRD was performed to study the purity and crystalline nature

of the nanoparticles. The morphological analysis was done by the Scanning Electron Microscopy (SEM) followed by elemental analysis by Energy-Dispersive-X-ray (EDAX) analysis. The crystal structure and phase transition of the nanoparticles were studied by Raman spectroscopy. The optical properties of the nanoparticles had measured using UV-Visible spectroscopy. The crystal structure and phase transition of the nanoparticles were studied by Raman spectroscopy. The optical properties of the nanoparticles had measured using UV-Visible spectroscopy. The s-parameters for EMI shielding effectiveness calculation was measured by vector network analyser using coaxial line method in 8-12GHz frequency range. The Shielding Effectiveness due to absorption (SE_A), due to reflection (SE_R) and total Shielding Effectiveness (SE) in terms of s-parameters is given by,

$$SE = 10\log(1/S_{21}^2)$$
$$SE_A = 10\log[S_{21}^2/(1-S_{11}^2)]$$
$$SE_R = 10\log(1-S_{11}^2)$$
$$SE = SE_A + SE_R$$

3. Results and Discussions

3.1. FTIR Analysis

The FTIR spectra for undoped Fe_3O_4 and nickel doped Fe_3O_4 is as shown in the Figure 1. The bands below 700cm^{-1} of Fe_3O_4 and Ni doped Fe_3O_4 attributed to the presence of pure Fe_3O_4 phase in the sample and also confirms the spinel structure of the crystalline samples[19,26] The broad bands at around 1543cm^{-1} and 3220cm^{-1} in both the samples represents the stretching and bending vibrations of -OH bonds of water and ethanol used in the synthesis of the samples. The bands at 452cm^{-1} and 457cm^{-1} of undoped and doped Fe_3O_4 is due to the octahedral stretching vibrations of the Fe-O bond. Also, 522cm^{-1} and 537cm^{-1} bands of the two samples show the tetrahedral stretching vibrations of Fe-O bond[29]. The slight shift in the bands represents the substitution of the Ni^{2+} into the octahedral site of the Fe_3O_4 spinel crystal structure which results in the variation of bond lengths of iron, nickel and oxygen[26]. Thus, the FTIR spectra supports the successful doping of nickel into the Fe_3O_4 crystal lattice.

3.2. XRD Analysis

The XRD patterns of the doped and undoped Fe_3O_4 is presented in the Figure 2. The XRD pattern of both the samples show the crystalline nature of the nanoparticles. The diffraction peaks in the undoped and doped Fe_3O_4 nanoparticles with miller indices (220), (311), (400), (511) and (440) are in agreement with the JCPDS data of the pure Fe_3O_4 nanoparticles

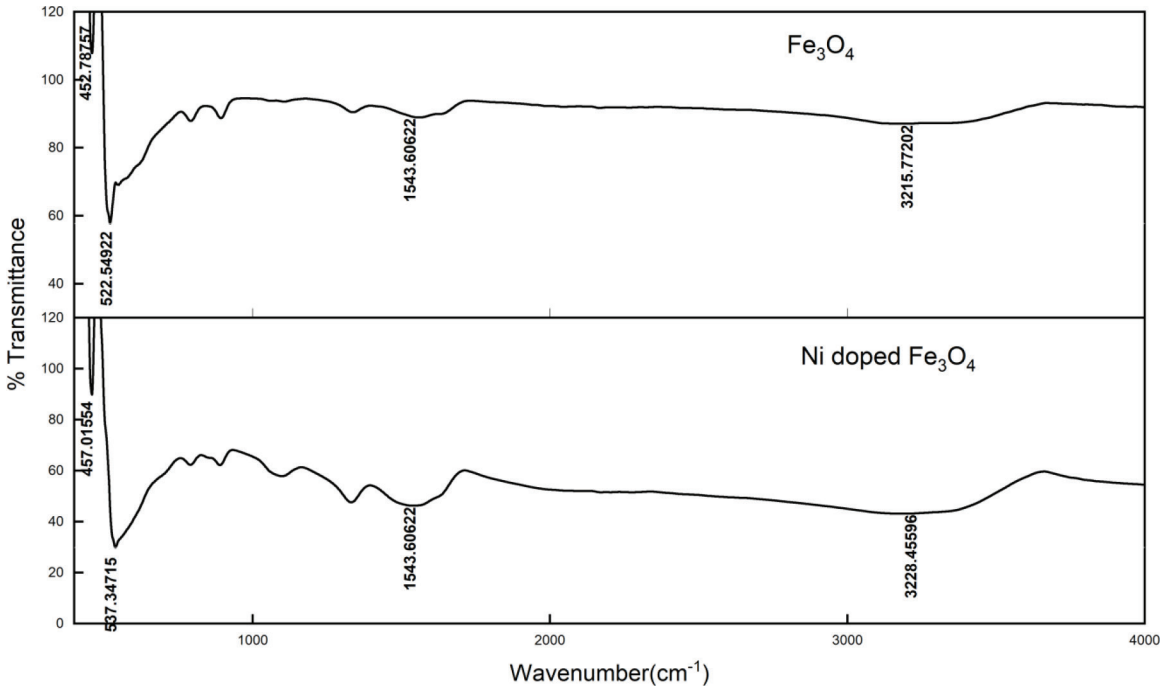


Figure 1. FTIR spectra of undoped and Ni-doped Fe_3O_4 nanoparticles.

with spinel structure[30]. This suggests the presence of the single phase of Fe_3O_4 in both the XRD patterns with no additional peaks for Ni-O and Ni, which in turn confirms the successful insertion of Ni^{2+} into the Fe_3O_4 matrix without altering its lattice structure[18,31]. This is attributed by the replacement of Fe^{2+} ions (r_{Fe}^{2+} = 73pm) by the Ni^{2+} ions (r_{Ni}^{2+} = 77pm) with almost same ionic radius into the octahedral site whereas Fe^{3+} ions are present in both octahedral and tetrahedral site of the crystal lattice[16]. Thus, the doping of Ni^{2+} into the Fe_3O_4 is confirmed by XRD analysis supported by FTIR and EDAX analysis.

3.3. Optical Properties

Optical properties such as absorbance and optical band gap have studied to investigate the characteristics of nanoparticles in UV-Visible region. The absorption spectra of Fe_3O_4 and the Ni doped Fe_3O_4 is as shown in the Figure 3. Both the nanoparticles witness the Similar absorption properties. Whereas, the small red shift is observed in Ni doped Fe_3O_4 nanoparticles (shift of absorption bands to longer wavelength region). This is owing to the free electrons in the Ni doped Fe_3O_4 leads to the delocalization in the nanoparticles.

The optical energy band gaps are calculated using Tauc Plots in which the linear region is extrapolated to the energy axis to get the Direct and Indirect band gaps. The Tauc Plots of undoped and doped Fe_3O_4 nanoparticles for direct and indirect energy band gap are depicted in Figure 4. The narrowing of band gap has observed in the Ni doped Fe_3O_4 for both direct and indirect band gaps as compared to undoped Fe_3O_4 interferes the doping of Ni^{2+} ions into the Fe_3O_4 matrix as the Ni^{2+} doping increases the impurity levels of the Fe_3O_4 nanoparticles which in turn decreases the energy band gap. Hence, the Ni doped Fe_3O_4 can be used in the photocatalytic application[26,32].

3.4. Raman Spectroscopy

Raman spectroscopy is viable method for structural elucidation of nanocrystals. This method gives clear information about the crystal structure, phase transition of the crystal and doping at the nano size compare to IR and XRD analysis[17,33,34]. The Raman spectra of the undoped and Ni doped Fe_3O_4 nanoparticles is shown in Figure 5. The spectra confirm the presence of single phase of Fe_3O_4 nanoparticles. The broadening in the peaks observed in the Ni doped Fe_3O_4 spectra indicates the doping of Ni^{2+} ions into the Fe_3O_4 matrix with minor modification in the spinel structure of Fe_3O_4 crystal lattice[23]. The undoped and Ni doped Fe_3O_4 spectra illustrate the five Raman active modes (E_g, A_{1g} and $3T_{2g}$) as explained by the Group Theory. These active modes confirm the spinel structure of both the nanoparticles, which belonging to the octahedral group. Thus, doping and crystal structure is clearly explained by Raman Spectroscopy.

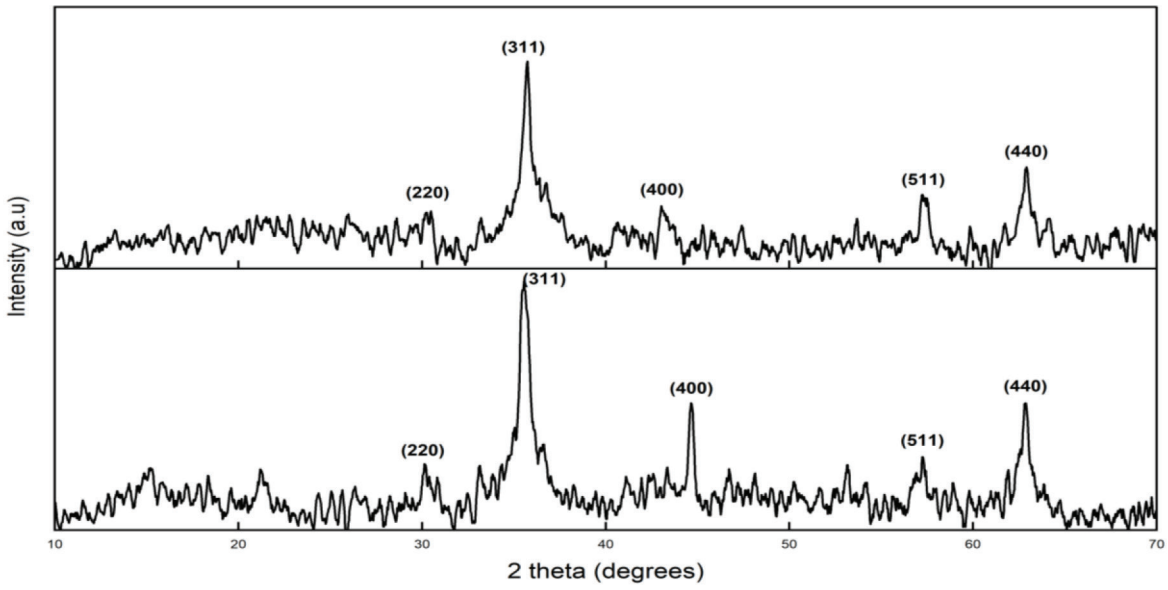


Figure 2. XRD patterns of undoped and Ni-doped Fe_3O_4 nanoparticles.

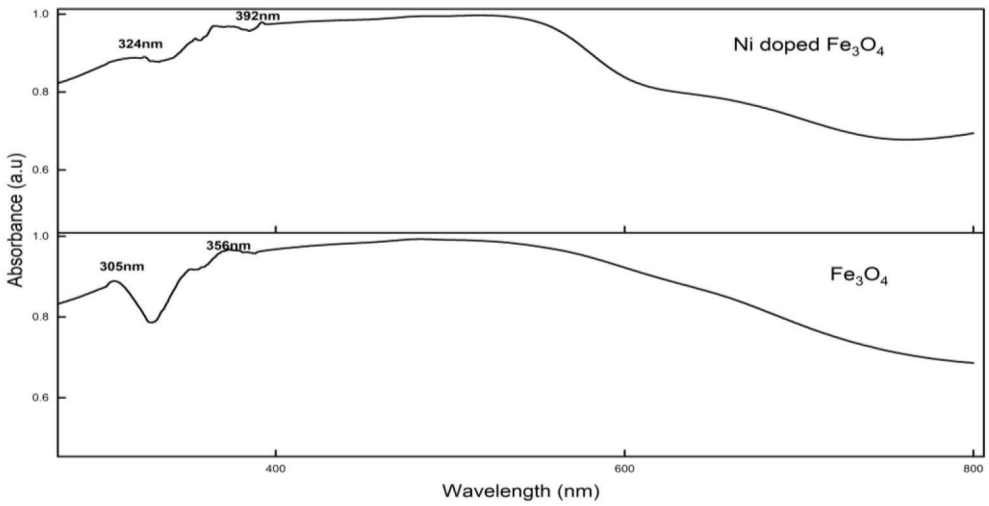


Figure 3. UV-Visible spectra of undoped and Ni-doped Fe_3O_4.

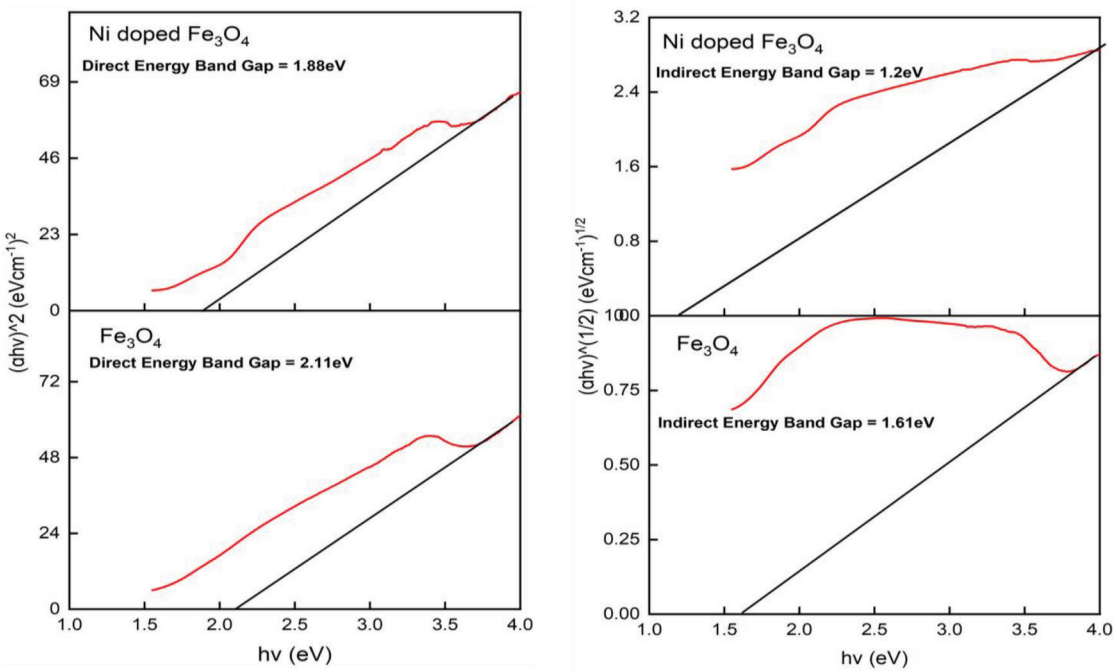


Figure 4. Tauc plots of undoped and Ni-doped Fe_3O_4 for direct and indirect energy band gaps.

3.5. SEM and EDAX Analysis

The SEM images of the Nickel doped Fe_3O_4 nanoparticle and its epoxy composites are as shown in Figure 3. The Ni doped Fe_3O_4 have the spherical shape and the agglomeration is due to the higher density of nickel on Fe_3O_4 nanoparticles, where Ni^{2+} ions lay on the top of the Fe_3O_4 crystal lattice. The spherical shape and uniform size of nanoparticles indicates the crystalline structure of the nanoparticles supported by XRD analysis[16,26,35].

Joundey *et al.* illustrate the better curing reaction of Ni-doped Fe_3O_4 than the undoped Fe_3O_4 by studying the curing kinetics of undoped Fe_3O_4 and Ni-doped Fe_3O_4 nanoparticles with epoxy resin. This is due to the Ni^{2+} ions on the top layer of Fe_3O_4 breaks the epoxy ring of the resin and increases the curing potential[35]. The SEM images of Ni-doped Fe_3O_4/epoxy composites show the good dispersion of nanoparticles into the epoxy matrix. As the filler content increases to 15wt%, the slight agglomeration

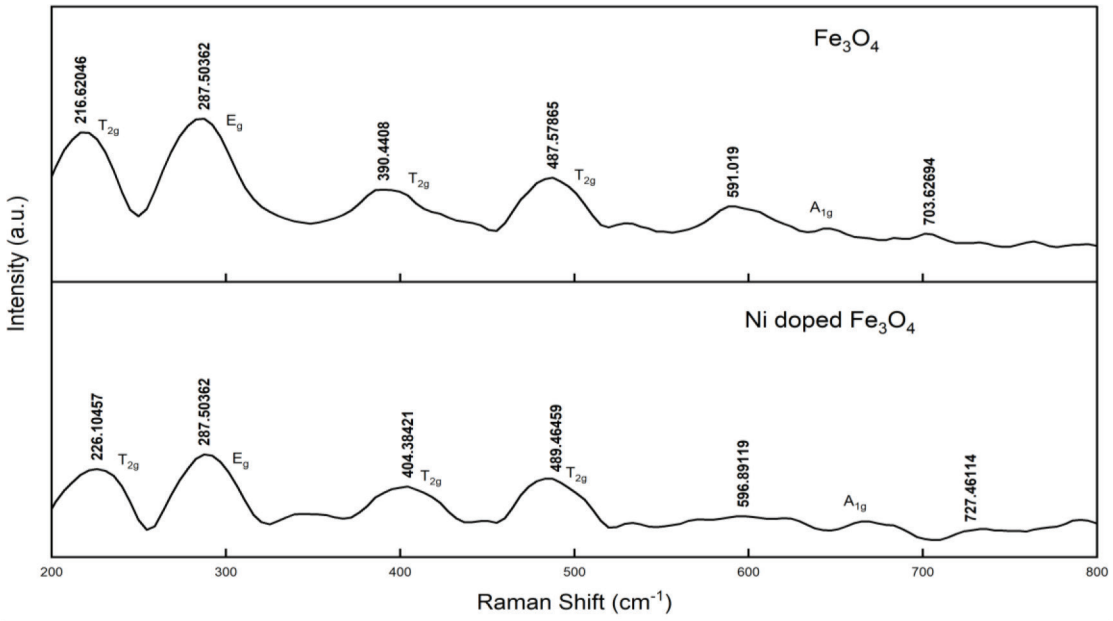


Figure 5. Raman spectra of undoped and Ni-doped Fe_3O_4 nanoparticles.

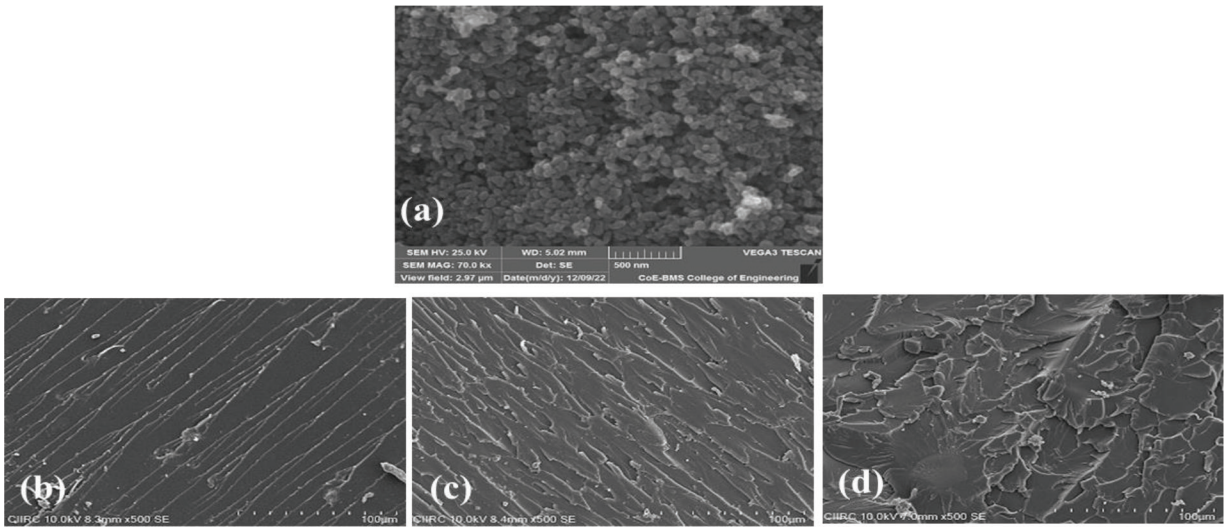


Figure 6. SEM images of (a) Ni Doped Fe_3O_4 (b) 5wt% Ni Doped Fe_3O_4/Epoxy Composite (c) 10wt% Ni Doped Fe_3O_4/Epoxy Composite (d) 15wt% Ni Doped Fe_3O_4/Epoxy Composite.

occurs due to the poor inter-facial bonding between the filler and the epoxy matrix.

The elemental analysis is performed to confirm the doping of Ni^{2+} into the Fe_3O_4 crystal lattice, which also gives quantitative elemental analysis present in the sample of the doped Fe_3O_4 by EDAX analysis is as shown in the Figure 4 which indicates the presence of elements such as Ni, Fe and O. This confirmed the formation of Ni doped Fe_3O_4 nanoparticles.

3.6. EMI SE Measurements

The S-parameters ($S_{11;}$the reflection coefficient and $S_{21;}$ the transmission coefficient) are recorded by the VNA in the X-band (frequency range of 8-12GHz). The EMI SE graph of Ni doped Fe_3O_4/epoxy composites is depicted in the Figure 8. As reported in the several literatures, EMI shielding is attributed by the magnetic losses, electric losses and electrical resistivity of the shielding material. The highest shielding effectiveness is shown in the15wt%

of Ni doped Fe_3O_4/epoxy composites (-24.46dB). The result is attributed by the increase in the magnetization of the polymer composites as Ni^{2+} ions occupy the crystal lattice and the saturation magnetization increases from 48.9emu to 115emu and becomes superparamagnetic in nature[18,19,23]. This in turn increases the magnetic permeability of the Ni doped Fe_3O_4/epoxy composites. The presence of Ni^{2+} ions also increase the conductivity of the composite due to the presence of free electrons. The Ni doped Fe_3O_4 also possess high dielectric losses and magnetic losses, which is very important in the EMI shielding process[21,22,24,29].

Also, the EMI SE value increases with the increase in the filler loading. The increase in the EMI SE value may be ascribed by the enhancement in the conductivity and dielectric properties of the Ni doped Fe_3O_4 nanoparticles. There is improvement in EMI SE value with the increase in the filler loading and is also illustrates the good inter-facial bonding between the filler and the epoxy resin supported by the SEM analysis. The 15wt% of Ni doped Fe_3O_4/epoxy composites show highest shielding effectiveness of -24.46dB at around 10GHz respectively. Hence, Ni doped Fe_3O_4/epoxy composites have become the prominent EMI shield in the X-frequency band.

The present work exhibited highest shielding effectiveness (-24.26dB) even with the low Ni^{2+} content; $Ni_{0.5}Fe_{2.5}O_4$/epoxy composite and the filler prepared by the simple co-precipitation method compared to the previously reported values.

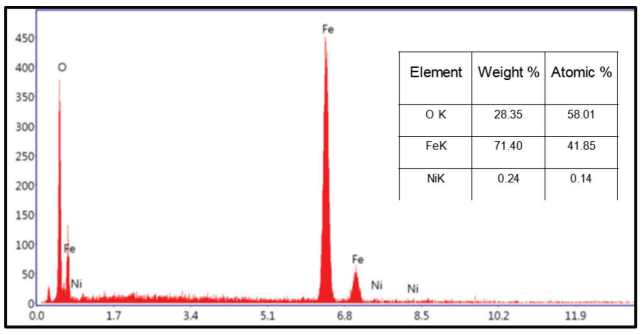


Figure 7. EDAX analysis of the Ni-doped Fe_3O_4 nanoparticles.

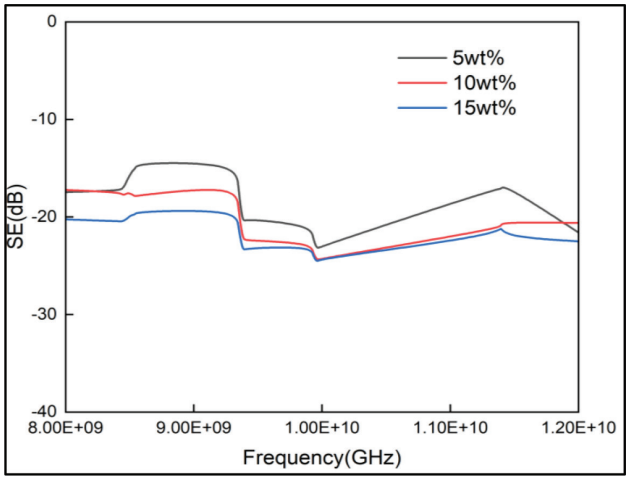


Figure 8. EMI SE graph of Ni doped Fe_3O_4.

4. Conclusion

The Ni doped Fe_3O_4 nanoparticles were prepared by the simple co-precipitation method as it is devoid the usage of advanced technology. The characterization was done using FTIR spectroscopy, XRD analysis, Raman spectroscopy, optical properties by UV-Visible spectroscopy, morphological studies using SEM, elemental analysis by EDAX and EMI shielding effectiveness measured using VNA in the X-band frequency range. The EMI studies showed that the EMI shielding properties increase with the increase in the filler loading which may be attributed due to the increase in conductivity and dielectric properties of Ni doped Fe_3O_4 nanoparticles. The 15wt% Ni doped Fe_3O_4/epoxy composite showed highest shielding effectiveness value of -24.46dB at 10GHz frequency range. The Ni doped Fe_3O_4/epoxy composite can be used for diverse applications with good optical and

Table 1. Comparison of EMI shielding properties of some recently reported Fe_3O_4/epoxy composites

Sl.No.	Composite	EMI SE (dB)	Reference
1	$Co_{0.6}Ni_{0.4}Fe_2O_4$	27	(21)
2	$NiFe_2O_4$	32.35	(2)
3	$NiFe_2O_4$/PANI-PTSA composite	22.31	(2)
4	1:3 Fe_3O_4: GNP/Epoxy composites	9.6	(36)
5	15wt% $Ni_{0.5}Fe_{2.5}O_4$/epoxy composite	-24.46	Present work

electrical properties. With high conductivity, magnetic and dielectric properties, the Ni doped Fe_3O_4/epoxy composites can be used as an eminent candidate for EMI shielding applications.

5. Acknowledgement

The Authors sincerely thank the VGST for financial support. We also extended our gratitude to RVCE for providing various facilities including the EMI shielding measurements.

6. References

1. Ali A, Hussain F, Tahir MF, Ali M, Zaman KM, Tomková B, *et al*. Fabrication of conductive, high strength and Electromagnetic Interference (EMI) shielded green composites based on waste materials. Polymers. 2022; 14(7):1289. https://doi.org/10.3390/polym14071289 PMid:35406163 PMCid: PMC9002487
2. Sulaiman JMA, Calinescu I. Electromagnetic Interference (EMI) shielding and microwave absorption properties of nickel ferrite $NiFe_2O_4$/ PANI-PTSA nanocomposite. Adv Mater Process Technol. 2020; 1-12. https://doi.org/10.1080/2374068X.2020.1856635
3. Nanotechnology in the Automotive Industry - 1st Edition [Internet]. [cited 2022 Oct 29]. Available from: https://www.elsevier.com/books/nanotechnology-in-the-automotive-industry/song/978-0-323-90524-4
4. Vishnumurthy KA, *et al*. Fabrication and comparison of mechanical and EMI shielding properties of various fibre reinforced multi-layered epoxy composites. J Indian Chem Soc. 2022; 99(10):100720. https://doi.org/10.1016/j.jics.2022.100720
5. Crespo Ribadeneyra M. EMI shielding composites based on magnetic nanoparticles and nanocarbons. 2014 Dec [cited 2022 Apr 20]; Available from: https://e-archivo.uc3m.es/handle/10016/20623
6. Geetha S, Satheesh KKK, Rao CRK, Vijayan M, Trivedi DC. EMI shielding: Methods and materials—A review. J Appl Polym Sci. 2009; 112(4):2073-86. https://doi.org/10.1002/app.29812
7. Banerjee P, Bhattacharjee Y, Bose S. Lightweight epoxy-based composites for EMI shielding applications. J Electron Mater. 2020; 49(3):1702-20. https://doi.org/10.1007/s11664-019-07687-5
8. Chandra RBJ, Shivamurthy B, Kulkarni SD, Kumar MS. Hybrid polymer composites for EMI shielding application-a review. Mater Res Express. 2019; 6(8):082008. https://doi.org/10.1088/2053-1591/aaff00
9. Ayub S, Guan BH, Ahmad F, Oluwatobi YA, Nisa ZU, Javed MF, *et al*. Graphene and iron reinforced polymer composite electromagnetic shielding applications: A review. Polymers. 2021; 13(15):2580. https://doi.org/10.3390/polym13152580 PMid:34372183 PMCid: PMC8347896
10. Liang C, Gu Z, Zhang Y, Ma Z, Qiu H, Gu J. Structural design strategies of polymer matrix composites for electromagnetic interference shielding: A review. Nano-Micro Lett. 2021; 13(1):181. https://doi.org/10.1007/s40820-021-00707-2 PMid:34406529 PMCid: PMC8374026
11. Ary Subagia IDG, Tijing LD, Kim Y, Kim CS, Vista IV FP, Shon HK. Mechanical performance of multiscale basalt fibre–epoxy laminates containing tourmaline micro/nanoparticles. Compos Part B Eng. 2014; 58:611-7. https://doi.org/10.1016/j.compositesb.2013.10.034
12. Wang L, Qiu H, Liang C, Song P, Han Y, Han Y, *et al*. Electromagnetic interference shielding MWCNT-Fe_3O_4@Ag/epoxy nanocomposites with satisfactory thermal conductivity and high thermal stability. Carbon. 2019; 141:506-14. https://doi.org/10.1016/j.carbon.2018.10.003
13. Chen W, Wang J, Zhang B, Wu Q, Su X. Enhanced electromagnetic interference shielding properties of carbon fibre veil/Fe_3O_4 nanoparticles/epoxy multiscale composites. Mater Res Express. 2017; 4(12):126303. https://doi.org/10.1088/2053-1591/aa9af9
14. Bhaskaran K, Bheema RK, Etika KC. The influence of Fe_3O_4@GNP hybrids on enhancing the EMI shielding effectiveness of epoxy composites in the X-band. Synth Met. 2020; 265:116374. https://doi.org/10.1016/j.synthmet.2020.116374
15. Xu J, Chen R, Yun Z, Bai Z, Li K, Shi S, *et al*. Lightweight epoxy/cotton fiber-based nanocomposites with carbon and Fe_3O_4 for electromagnetic interference shielding. ACS Omega. 2022; 7(17):15215-22. https://doi.org/10.1021/acsomega.2c01293 PMid:35572748 PMCid: PMC9089691
16. Cure kinetics of samarium-doped Fe_3O_4/epoxy nanocomposites - abstract - Europe PMC [Internet]. [cited 2023 Jan 19]. Available from: https://europepmc.org/article/ppr/ppr429793
17. Gupta R, Sood AK, Metcalf P, Honig JM. Raman study of stoichiometric and Zn-dopedFe_3O_4. Phys Rev B. 2002; 65(10). https://doi.org/10.1103/PhysRevB.65.104430
18. Aghazadeh M, Karimzadeh I, Ganjali MR. Dextran grafted nickel-doped superparamagnetic iron oxide nanoparticles: Electrochemical synthesis and characterization. J Nanostructures. 2019; 9(3):531-8.
19. Larumbe S, Gómez-Polo C, Pérez-Landazábal JI, García-Prieto A, Alonso J, Fdez-Gubieda ML, *et al*. Ni-doped Fe_3O_4 magnetic nanoparticles. J Nanosci Nanotechnol. 2012; 12(3):2652-60. https://doi.org/10.1166/jnn.2012.5769 PMid:22755104
20. Muhammad AJ. Synthesis and characterization of nickel-doped iron oxide nanoparticles for biomedical application.

21. Electromagnetic interference shielding and characterization of Ni_{2+} substituted cobalt nano ferrites prepared by Sol-Gel auto combustion method. [cited 2023 Jan 18]. Available from: https://doi.org/10.1155/2022/3992402
22. Moharana A, Kumar D, Kumar A. Synthesis of Ni-doped iron oxide nanoparticles and their dielectric properties. J Phys Conf Ser. 2020; 1531(1):012113. https://doi.org/10.1088/1742-6596/1531/1/012113
23. Deepak FL, Bañobre-López M, Carbó-Argibay E, Cerqueira MF, Piñeiro-Redondo Y, Rivas J, *et al*. A systematic study of the structural and magnetic properties of Mn-, Co-, and Ni-doped colloidal magnetite nanoparticles. J Phys Chem C. 2015; 119(21):11947-57. https://doi.org/10.1021/acs.jpcc.5b01575
24. Moharana A, Kumar D, Kumar A. Synthesis of Ni-doped iron oxide nanoparticles and their dielectric properties. J Phys Conf Ser. 2020; 1531(1):012113. https://doi.org/10.1088/1742-6596/1531/1/012113
25. Pal Singh S, Kumari Singh A, Gupta J. Synthesis of nickel-doped iron oxide nanoparticles by co-precipitation method and investigation of its structural and optoelectronic properties. Mater Today Proc. 2022; 66:1890-6. https://doi.org/10.1016/j.matpr.2022.05.415
26. Kamakshi T, Sunita SG, Erothu H, Subhakaran SR. Effect of nickel dopant on structural, morphological and optical characteristics of Fe_3O_4 nanoparticles. Rasayan J Chem. 2019; 12(02):531-6. https://doi.org/10.31788/RJC.2019.1225054
27. Mohanraj K, Sivakumar G. Synthesis of γ-Fe2O3, Fe_3O_4 and copper doped Fe_3O_4 nanoparticles by sonochemical method. Sains Malays. 2017; 46(10):1935-42. https://doi.org/10.17576/jsm-2017-4610-32
28. Zhang X, Alloul O, Zhu J, He Q, Luo Z, Colorado HA, *et al*. Iron-core carbon-shell nanoparticles reinforced electrically conductive magnetic epoxy resin nanocomposites with reduced flammability. RSC Adv. 2013; 3(24):9453-64. https://doi.org/10.1039/c3ra41233d
29. Saleem A, Zhang Y, Gong H, Majeed MK, Lin X, Hussain MM, *et al*. Electromagnetic wave absorption performance of Ni-doped Cu-ferrite nanocrystals. Mater Res Express. 2020; 7(1):016117. https://doi.org/10.1088/2053-1591/ab6c1a
30. Muhammad AJ. Synthesis and characterization of nickel-doped iron oxide nanoparticles for biomedical application.
31. Electrochemical sensing behaviour of Ni-doped Fe_3O_4 nanoparticles: AIP Conference Proceedings: Vol 1576, No 1 [Internet]. [cited 2023 Jan 19]. Available from: https://aip.scitation.org/doi/10.1063/1.4861998
32. Photocatalytic activity of Ni Doped Fe_3O_4, Fe_3O_4/GO, and Fe_3O_4/rGO nanocomposite materials - Google Search [Internet]. [cited 2023 Jan 19]. Available from: https://www.google.com/search?q=PHOTOCATALYTIC+ACTIVITY+OF+Ni++DOPED+Fe_3O_4,+Fe_3O_4/GO,+AND+Fe_3O_4/rGO++NANOCOMPOSITE+MATERIALSandsource=lmnsandbih=656andbiw=1396andrlz=1C1CHBF_enIN944IN944andhl=enandsa=Xandved=2ahUKEwji_9OJo9L8AhXM23MBHYQRBnIQ0pQJKAB6BAgBEAI
33. Testa-Anta M, Ramos-Docampo MA, Comesaña-Hermo M, Rivas-Murias B, Salgueiriño V. Raman spectroscopy to unravel the magnetic properties of iron oxide nanocrystals for bio-related applications. Nanoscale Adv. 2019; 1(6):2086-103. https://doi.org/10.1039/C9NA00064J PMid:36131987 PMCid: PMC9418671
34. Short-Range B-site ordering in inverse spinel ferrite $NiFe_2O_4$ [Internet]. [cited 2023 Jan 19]. Available from: https://www.researchgate.net/publication/235547742_Short-Range_B-site_Ordering_in_Inverse_Spinel_Ferrite_$NiFe_2O_4$/figures?lo=1andutm_source=googleandutm_medium=organic
35. Curing epoxy with electrochemically synthesized $NixFe_3$-xO_4 magnetic nanoparticles - ScienceDirect [Internet]. [cited 2023 Jan 19]. Available from: https://www.sciencedirect.com/science/article/pii/S030094401930709X
36. Bhaskaran K, Bheema RK, Etika KC. The influence of Fe_3O_4@GNP hybrids on enhancing the EMI shielding effectiveness of epoxy composites in the X-band. Synth Met. 2020; 265:116374. https://doi.org/10.1016/j.synthmet.2020.116374